International Journal of Environmental Science and Technology (2023) 20:4127–4138
https://doi.org/10.1007/s13762-022-04118-7

ORIGINAL PAPER

Effective dose estimation of radon, thoron and their progeny concentrations in the environs of Himalayan belt, India

P. Semwal[1] · T. K. Agarwal[2] · M. Joshi[2] · A. Kumar[3] · K. Singh[1] · R. C. Ramola[4]

Received: 17 June 2021 / Revised: 20 November 2021 / Accepted: 13 March 2022 / Published online: 18 April 2022

Abstract

Studies on the measurement of ^{222}Rn, ^{220}Rn and their decay product's concentration level are important as they are the significant contributor to background radiation dose. This study presents results of measurements conducted in 80 houses situated in Nainital District of Kumaun Himalayan region, Uttarakhand, India. Single entry-based pin hole dosimeters and direct ^{222}Rn progeny sensors/direct ^{220}Rn progeny sensors were used to measure the concentrations of ^{222}Rn and ^{220}Rn, and their decay products. Estimation of yearly averaged summary parameters and the effect of different types of building materials (mud, stone and cement) and seasonal variations (winter, summer and rainy) have been done. The role of ventilation and source term towards the observed variations has been interpreted. It was seen that in most of the mud houses of the study region, gases and their decay product's concentration remained significantly higher than their respective global average in the winter season. Annual inhalation dose due to ^{222}Rn, ^{220}Rn and their progeny was found to be 0.85–3.93 mSv with GM (GSD) as 1.71 (1.76) mSv. The present study showed that a significant contribution to annual inhalation dose comes from ^{220}Rn and its decay products. The findings in-line to the recent studies conducted in Indian Himalayan region and add strength to the existing database.

Keywords Seasonal variation · Building materials · Inhalation dose · Radon · Thoron · Decay products

Introduction

It is well known that the radionuclides ^{222}Rn (radon) and ^{220}Rn (thoron), and their decay products contribute ~ 50% of natural background dose to humans (UNSEAR 2000; UNSCEAR 2010). This fraction further increases in radium/thorium handling facilities and poorly ventilated buildings (IAEA 2005; WHO 2009). Being particulates in nature, decay products deposit into the lungs resulting in an increase in inhalation radiation exposure. This may lead to DNA damage resulting in induction of cancer for prolonged exposure scenarios (ICRP 2014; UNSCEAR 2000; WHO 2009). The enhanced lung cancer risk came out to be 8% (3–16%) per 100 Bq/m^3 of radon concentration (Darby et al. 2005) in case–control studies conducted in Europe. Studies estimated in cold weather region relation to socio-economic factors including fuel poverty, and the role of thermally inefficient housing such inhalation risk in terms of lung cancer incidences and/or frequency of deaths. For example, Milner et al. 2014 estimated approximately 1100 deaths per year due to the exposure of ^{222}Rn and ^{220}Rn in the UK. Radon was also attributed to 300 instances of lung cancer in the dwellings of Ireland every year (Dowdall et al. 2017). Several such studies conducted in different regions worldwide have established the link between the indoor ^{222}Rn and ^{220}Rn exposure to the detrimental effects on human health (Krewski et al. 2005; Wang and Ward 2002).

Profiling of ^{222}Rn, ^{220}Rn and their decay concentration via short-term and continual measurements for both residential areas and occupational buildings has been an active research domain in last few decades. This has increased

Editorial responsibility: I. Akkurt.

✉ P. Semwal
poonamsemwal05@gmail.com

[1] Department of Physics, Govt. P.G. College, Tehri Garhwal, New Tehri 249001, India

[2] Radiological Physics and Advisory Division, Bhabha Atomic Research Center, Mumbai 400094, India

[3] Department of Physics, Gurukula Kangri Vishwavidyalaya, Haridwar 249404, India

[4] Department of Physics, HNB, Garhwal University, Badshahi Thaul Campus, Tehri Garhwal, Srinagar 249199, India

the level of understanding of research community and has futuristic implications in terms of reformed building designs for the policy makers. Ambient factors such as the effect of environmental characteristics, viz. seasons, ventilation, source-term, etc. affect the levels of ^{222}Rn, ^{220}Rn and their decay products considerably (Agarwal et al., 2019; Joshi et al. 2011; Hu et al. 2018; Kumar et al. 2020a, b; Kumara et al. 2017; Mishra et al. 2014; Omori et al. 2020; Semwal et al. 2019). This becomes more crucial for a country like India where the diverse conditions of climate, geology and socio-economy tend to intensify the role of studies in different regions culminating towards a meaningful scientific interpretation. This led to perform several studies and efforts to form a statistically sound database useful for the future applications (Bangotra et al. 2016; Karunakara et al. 2014, 2020; Prasad et al. 2018b; Meisenberg et al. 2016; Ramola and Prasad 2020; Sahoo et al. 2011). Geological conditions (Ramola et al. 2013), dwelling types (Sharma et al. 2018; Semwal et al. 2019) and seasonal variations (Bangotra et al. 2019; Prasad et al. 2016a) have been shown to be affecting the concentration levels of ^{222}Rn/^{220}Rn gases and decay products. In addition to the measurements, the efforts in terms of development of various numerical and analytical models (Sahoo et al. 2011; Shetty et al. 2020; Trilochana et al. 2020; Agarwal et al. 2014, 2015, 2020) has helped to enhance the knowledge relatable to different issues/contexts.

The Indian Himalayan belt has unique features regarding the geology, climate, neo-tectonic, faults and geophysical activities (Singh et al. 2016; Semwal et al. 2018, 2019; Prasad et al. 2016b; Ramola et al. 2013, 2016). Few recent studies on the measurements of indoor ^{222}Rn/^{220}Rn and decay products in Indian Himalayan belt highlighted the higher levels and associated the contributing factors with the observed data (Kandari et al. 2018; Prasad et al. 2018a; Prasad et al. 2008; Semwal et al. 2018, 2019). This work discusses the experimental measurements of indoor ^{222}Rn, ^{220}Rn and their decay product activity levels performed in Nainital District of Uttarakhand, India. Closeness to the seismic fault layer, unique rock and soil characteristics and cold climatic conditions necessitated the formulation of this campaign. Measurements were taken in 80 houses selected from the study region on defined pre-campaign basis. The results have been presented and the estimations of yearly averaged parameters have been made in this work.

Topography of the studied area

The Nainital District selected for the present study is situated in Kumaon region of Indian Himalayan belt, located between coordinates 80° 14'–78° 80' E and 29° 00'–29° 05' N with an elevation of 424–2084 m from the sea level (shown in Fig. 1). Due to its locations and pleasant climate conditions, Nainital remains an attractive place for tourists throughout the year. The Nainital hills represent the south eastern part of a strip of enechelon basins of the Krol belt, which stretches south eastward from Solan (Himachal) to Nainital (Uttarakhand). The rock mainly comprises of garnet-ferous mica-schits, which contains layers of quartzites, lenses of graphite schists and band of gneissic rocks (Sinha 1977). The southern limit of the Krol belt is delineated by the highly tectonized rocks of the Amritpur granites (Valdiya 1980), which have been brought up along Main Boundary Thrust (MBT). Quartzites, graphite, etc. are the prime sources of Uranium and Thorium.

Details of the selected dwellings

A pre-survey for outdoor gamma radiation level (using ATOMTEX Gamma radiation survey meter) was conducted in the Nainital District. As a result, the studied region was segregated into two different zones as shown in Table 1. There were prominently three types of construction of the houses in the studied region. Type A represents the mud houses (mud and wood), type B stands for the stone houses (stone with cement plaster) and type C is cement houses (bricks and coated with cement). In this way, total 80 houses are selected for carrying out elaborative indoor measurements. The respective distribution of number of houses is shown in Table 1. A satellite-based GARMIN GPS; ETREX-10 monitor was used to determine the topography (latitude, longitude and altitude) of the selected houses.

Materials and methods

Measurement of gas concentration

The ^{222}Rn and ^{220}Rn concentration was measured using "single entry face Pin-hole dosimeter" aboriginal designed by Bhabha Atomic Research Centre (BARC), Mumbai (Sahoo et al. 2013). Figure 2 shows a schematic illustration of the dosimeter used for the measurement. Two chambers of the dosimeter are detached by a central pinhole disc, which segregates ^{220}Rn from ^{222}Rn. Both cylindrical chamber measures 4.1 cm in length and 3.1 cm in radius. The foremost chamber determines ^{222}Rn + ^{220}Rn while the second chamber determines the ^{222}Rn only. The gas accesses ^{222}Rn + ^{220}Rn chamber through a filter paper made of glass fiber (to cut-off the entry of their decay products), which is placed at the entry face and subsequently diffuses to ^{222}Rn chamber. The LR-115 Type-II detector films of 3 cm × 3 cm are pre-fixed in these chambers to register the alpha tracks generated by ^{222}Rn, ^{220}Rn and their decay products. The unbiased electric field is maintained inside the chamber by metal powder

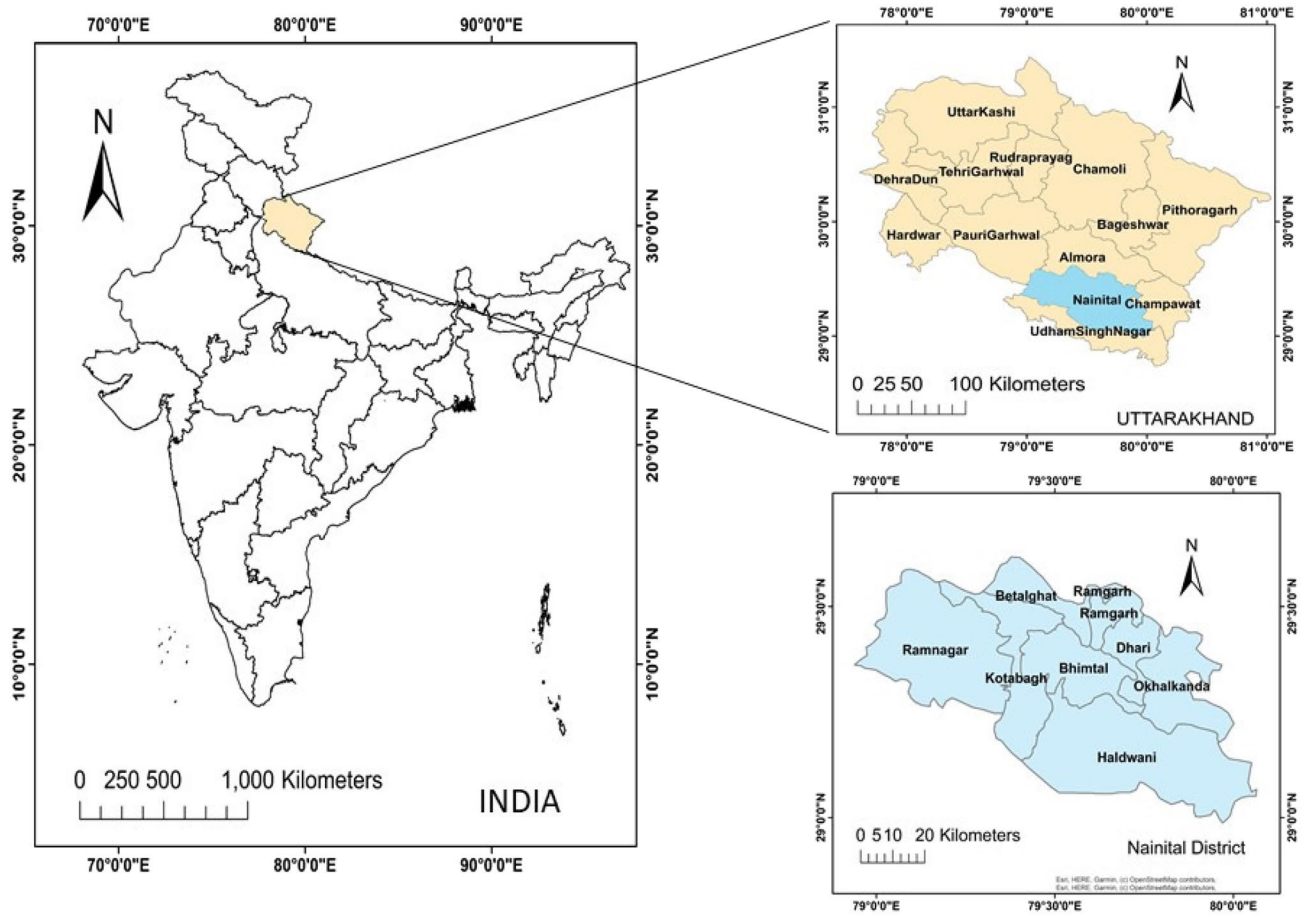

Fig. 1 Nainital District Map for measurements

Table 1 Distribution of houses with respect to the type of construction and gamma zone

S. No	Gamma level (μSv/y)	Type of houses		
		A	B	C
1	0.11–0.20	16	14	40
2	0.21–0.30	3	3	4

coating for facilitating the uniform deposition of decay products. The comprehensive study of the measurement technique and its determination and validation of pin-hole dosimeter are reported by Sahoo et al. (2013).

Determination of the concentration of decay products

The decay product of ^{222}Rn and ^{220}Rn was measured using Direct ^{222}Rn Progeny Sensor (DRPS) and Direct ^{220}Rn Progeny Sensor (DTPS), aboriginal made by BARC, Mumbai (Mishra et al. 2009a; b). The schematic diagram of the direct

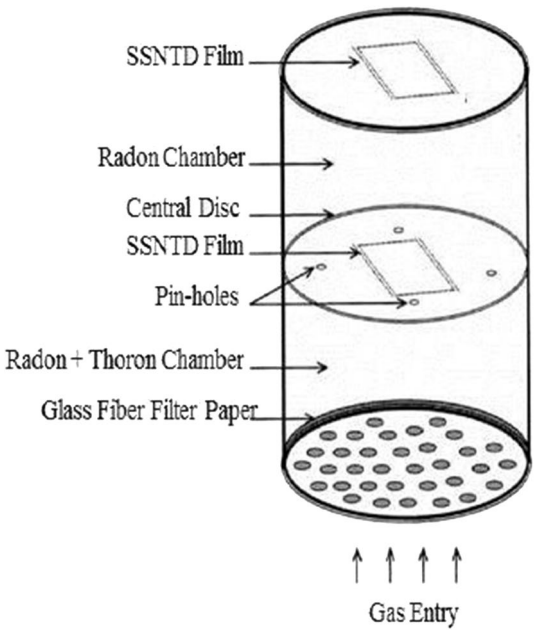

Fig. 2 Schematic diagram of single entry pin-hole dosimeter

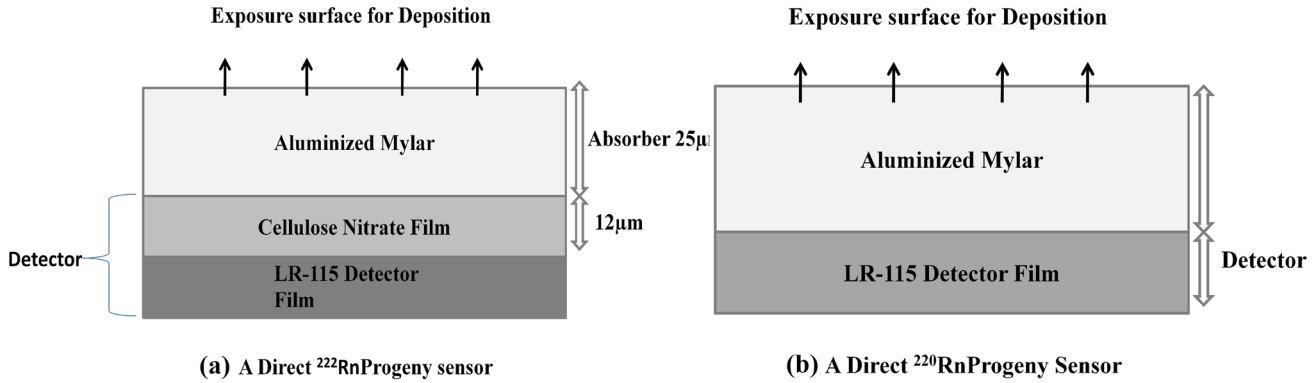

Fig. 3 The schematic diagram of direct ^{222}Rn/^{220}Rn progeny sensors (DRPS/DTPS)

progeny sensing system is shown in Fig. 3. DRPS and DTPS are composed of LR115 detector foil and aluminized polyester film, arranged in a cassette. Selected polyester film thickness of 37 microns and 50 microns is used to record tracks in DRPS and DTPS due to the alpha particles emission from ^{214}Po (α energy 7.69 MeV) and ^{212}Po (α energy 8.78 MeV) for the detection of ^{222}Rn decay products. Whereas the tracks generated by the ^{212}Po (α energy 8.78 MeV) are registered to detect the ^{222}Rn decay products. The recorded tracks are used to estimate the equilibrium equivalent concentration of the ^{222}Rn and ^{220}Rn decay products present in the surrounding air. A detailed description of the measurement technique, calibration and validation is found elsewhere (Mishra et al. 2010, 2009a, b; Mishra and Mayya 2008a, b). The dosimeter and DTPS/DRPS are commonly used in the numerous studies at various locations worldwide. (Bajwa et al. 2016; Singh et al. 2016; Mishra et al. 2014; Ramola et al. 2016).

Evaluation of equilibrium factors

Equilibrium equivalent concentration (EEC) of ^{222}Rn/^{220}Rn is equal to that quantity of ^{222}Rn/^{220}Rn which is in secular equilibrium with its decay products giving equivalent potential alpha energy concentration (PAEC) for the decay products present in the environment. Thus, the equilibrium factor is defined as the ratio of EERC/EETC to the ^{222}Rn/^{220}Rn concentration in the atmosphere. The equilibrium factors for ^{222}Rn (F_{Rn}) and ^{220}Rn (F_{Tn}) can be calculated using Eqs. (1 and 2).

$$F_R = \frac{\text{EERC}}{C_R} \tag{1}$$

$$F_T = \frac{\text{EETC}}{C_T} \tag{2}$$

where C_R and C_T are the concentrations of ^{222}Rn and ^{220}Rn, respectively.

Assessment of total annual inhalation and annual effective dose

The total annual inhalation dose (D) and the annual effective dose (AED) due to exposure of indoor ^{222}Rn, ^{220}Rn and their decay products have been calculated using Eqs. (3–5) as given by UNSCEAR (2000).

$$\begin{aligned} D(\text{mSv}/y) = {} & \{(0.17 + 9 \times F_R)xC_R \\ & + (0.11 + 40 \times F_T) \times C_T\} \\ & \times 8760 \times 0.8 \times 10^{-6} \end{aligned} \tag{3}$$

$$\begin{aligned} \text{AEDR}(\text{mSv}/y) = {} & \text{EERC}(\text{Bq}/m^3) \times 8760h \\ & \times 0.8 \times 9\text{nSv}(\text{Bq} \cdot h/m^3)^{-1} \times 10^{-6} \end{aligned} \tag{4}$$

$$\begin{aligned} \text{AEDT}(\text{mSv}/y) = {} & \text{EETC}(\text{Bq}/m^3) \times 8760h \\ & \times 0.8 \times 40\text{nSv}(\text{Bq} \cdot h/m^3)^{-1} \times 10^{-6} \end{aligned} \tag{5}$$

The dose conversion coefficients for the concentration of ^{222}Rn and its decay products are 0.17 and 9, respectively; whereas 0.11 and 40 are the dose conversion factors for ^{220}Rn and its decay products concentrations (UNSCEAR 2000). 0.8 is the indoor occupancy factor for 1 year exposure period (UNSCEAR 1993). 10^{-6} is the multiplication factor for unit conversion from nSv to mSv.

Results and discussion

Effect of seasonal variation on dose estimation

To observe the seasonal effects, dosimeters were deployed in the dwellings for a block period of four months (i.e. November–February, March–June and July–October), representing the three successive seasons (winter, summer, rainy) in a year. Seasonal classification has been done

based on environmental parameters (temperature and relative humidity) and houses features (e.g. ventilation rate) which vary with the seasons.

The Q–Q plots (probability plots) are used to show the statistical distribution of data around their mean. If the data in the Q–Q plot lie on a straight diagonal line with minimal deviations, it indicates the normal distribution. Figure 4 gives Q–Q plots of ^{222}Rn and ^{220}Rn concentration during winter, summer and rainy seasons. In statistics, skewness is a measure of symmetry, or more precisely, degree of asymmetry. A distribution/data set is symmetric(mean = mode = median) if it looks the same to the left and right of the center point and Kurtosis is a measure of the combined weight of a distribution's tails relative to the center of the distribution. Positively Skewed Distribution is a type of distribution where the mean, median, and mode of the distribution are positive rather than negative or zero. As can be observed, data for ^{222}Rn and ^{220}Rn is showing a rightly skewed pattern for all seasons, e.g. winter (Sk = 0.52 and 0.86), summer (Sk = 0.35, Sk = 0.92) and rainy (Sk = 0.86; Sk = 0.48) season; indicating a log-normal distribution with right tail. EERC and EETC also followed the same pattern in all three seasons as observed for their parent gases. As ^{222}Rn, ^{220}Rn and their decay products concentration pattern follow a log-normal distribution, it is therefore recommended to representing the data with a geometric mean (GM, GSD) rather than arithmetic mean (AM ± SD). It is to avoid the biasing or inclination of the results towards a larger or smaller data value in the distribution.

The statistical parameters such as range, geometric mean (GM), geometric standard deviation (GSD), relative standard deviation (RSD), skewness (Sk) and kurtosis (K) explaining the effect of seasonal variation on ^{222}Rn, ^{220}Rn and EERC-EETC concentration are tabulated in Table 2. GM for ^{222}Rn were found to be varying in order of winter > summer > rainy. While the dispersion parameters (RSD and GSD) are seen to be comparable for different seasons. A similar distribution pattern can be noticed for EERC also. On the other hand, ^{220}Rn and EETC profiles are quite dissimilar to each other as expected. This is because of ^{220}Rn concentration profile is not observed to be affected by the existing ventilation rate in the region due to its short half-life. However, seasonal effect can be clearly seen on EETC due to the longer half-life of decay products. It is also evident from Table 2 that mean values in winter season for ^{222}Rn, ^{220}Rn and EERC-EETC concentration can be observed marginally higher than that of summer and rainy season. This indicates 'offset ventilation effect', i.e. smaller difference for winter and summer season because of ventilation patterns of cold regions, doors and windows, are opened during

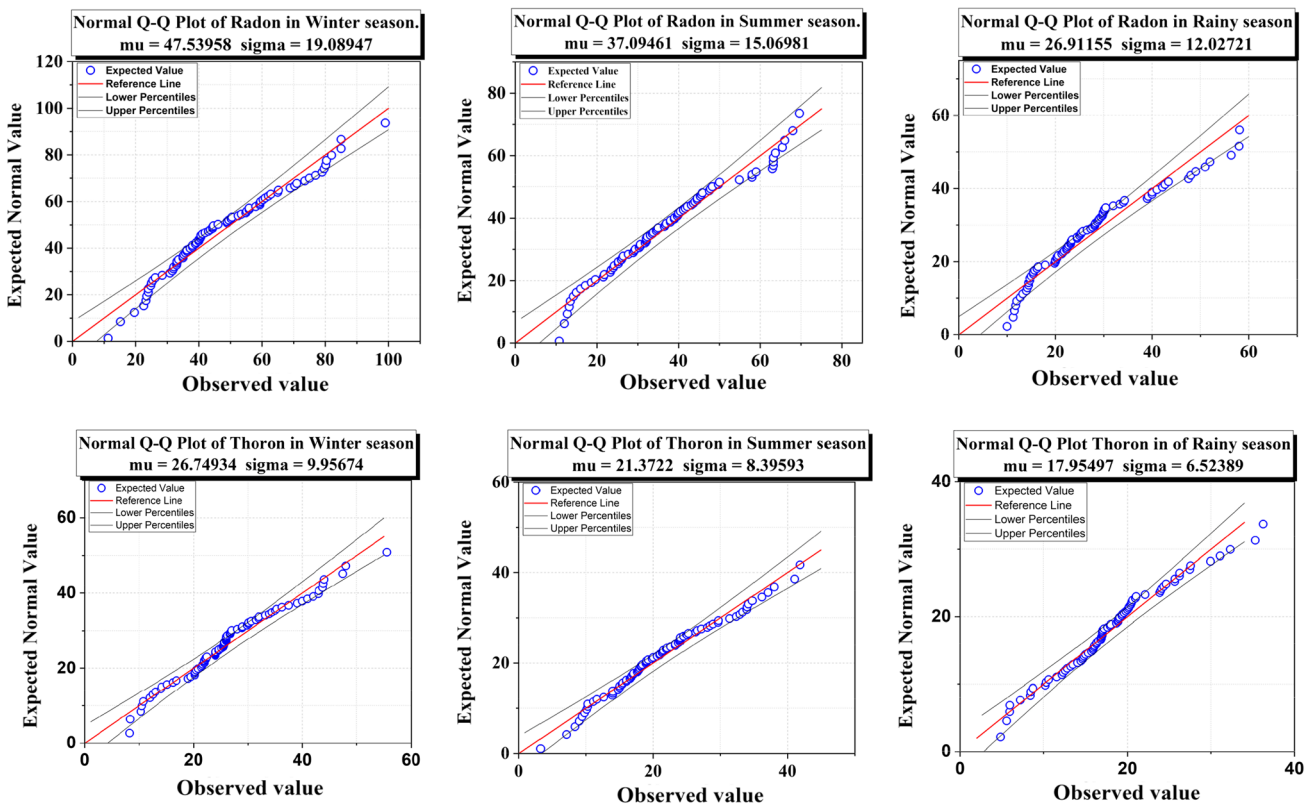

Fig. 4 Q–Q probability plots for ^{222}Rn, ^{220}Rn

daytime in winters to allow warm sunlight inside dwellings and makes ventilation rates for summers (where air mixing is higher) and winters comparatively similar, which is a common occurrence in most Indian studies conducted in cold climates (Semwal et al. 2019). As water fills the pores of the soil, the exhalation potential decreases, influencing the emission from building materials in damp conditions; resulting lower concentration of ^{222}Rn, ^{220}Rn and their respective decay products in the rainy season than compared to winter and summer (Bangotra et al. 2019; Kaur et al. 2018; Semwal et al. 2019).

To further investigate the seasonal effect, pie charts for ^{222}Rn and ^{220}Rn are presented in Fig. 5. Figure 5 indicates that ~ 68% of the houses in the winter season showed the indoor ^{222}Rn concentration higher than the global average (40 Bq/m^3). While, this fraction reduces to ~ 41% and 17.5% in summer and rainy season, respectively, as expected. It can also be noticed that ^{222}Rn concentration reach greater than 100 Bq/m^3 (reference value, WHO) in 8.75% of the houses in winter season (only). For EERC, 63%, 36% and 20% the houses in the winter, summer and rainy season, respectively, were reported to have a concentration higher than its yearly average of 21 Bq/m^3 (discussed in Implication from yearly data section).

On the other hand, ^{220}Rn and EETC concentrations were found to be significantly higher than their global average of 10 Bq/m3 and 0.02 Bq/m3, respectively, in the studied region. For the case of ^{220}Rn, 56% and 56% and 47% of the houses in winter, summer and rainy season, respectively, showed ^{220}Rn concentration higher than its annual average of 34 Bq/m^3 (discussed in Implication from yearly data section). While 2.5%, 1.25% of the houses were observed having ^{220}Rn concentration higher than 100 Bq/m^3 (arbitrary reference) in winter and summer season. EETC concentration was observed higher than its yearly average of 0.58 Bq/m^3 (discussed in Implication from yearly data section) in 63%, 40%, 41% the houses in winter, summer and rainy seasons, respectively.

Influence of building material

The effects of construction material qualities (radioactivity content, grain size, porosity, etc.) on indoor concentration levels are well documented (Prajith et al. 2019). The effect of building material on the distribution pattern of ^{222}Rn and ^{220}Rn has also been studied and the annual data has been segregated based on the building types (Mud, Stone and Cement). Detectors were exposed in each of these homes during all three seasons, resulting in three readings for each dwelling over the course of a year. The distribution of ^{222}Rn, ^{220}Rn, EERC and EETC for this case has been illustrated in Fig. 6a, b and statistical parameters are given in Table 3.

Table 2 Statistical data of seasonal variation for indoor ^{222}Rn, ^{220}Rn of Nainital district

Statistical parameters	^{222}Rn (Bq/m^3)			^{220}Rn(Bq/m^3)			EERC(Bq/m^3)			EETC(Bq/m^3)		
	W	S	R	W	S	R	W	S	R	W	S	R
Range	11–99	11–70	9–58	10–120	10–110	6–90	8–56	3–42	5–36	0.13–4.42	0.04–3.96	0.03–3.70
RSD	0.41	0.41	0.44	0.60	0.49	0.50	0.37	0.39	0.36	0.90	1.20	1.03
GM, GSD	43, 1.53	34, 1.57	24, 1.56	36, 1.89	35, 1.69	32, 1.73	25, 1.52	20, 1.56	17, 1.51	0.93, 2.82	0.61, 3.56	0.40, 3.28
Skewness	0.52	0.35	0.86	0.86	0.92	0.93	0.48	0.40	0.45	0.75	1.47	1.25
Kurtosis	–0.39	–0.51	0.19	0.33	1.50	1.32	0.13	–0.27	0.55	–1.00	1.13	1.37

W winter, *S* summer, *R* rainy

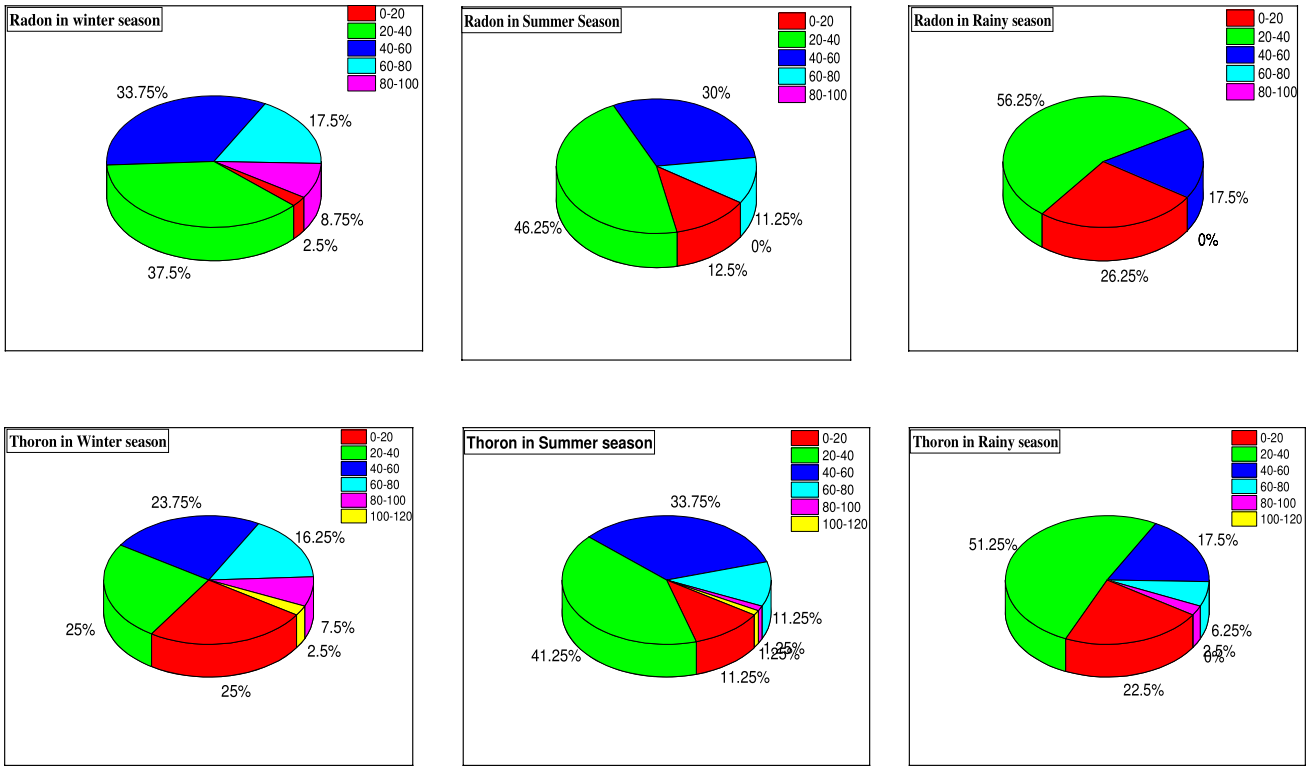

Fig. 5 The seasonal variation Pie chart of ^{222}Rn and ^{220}Rn

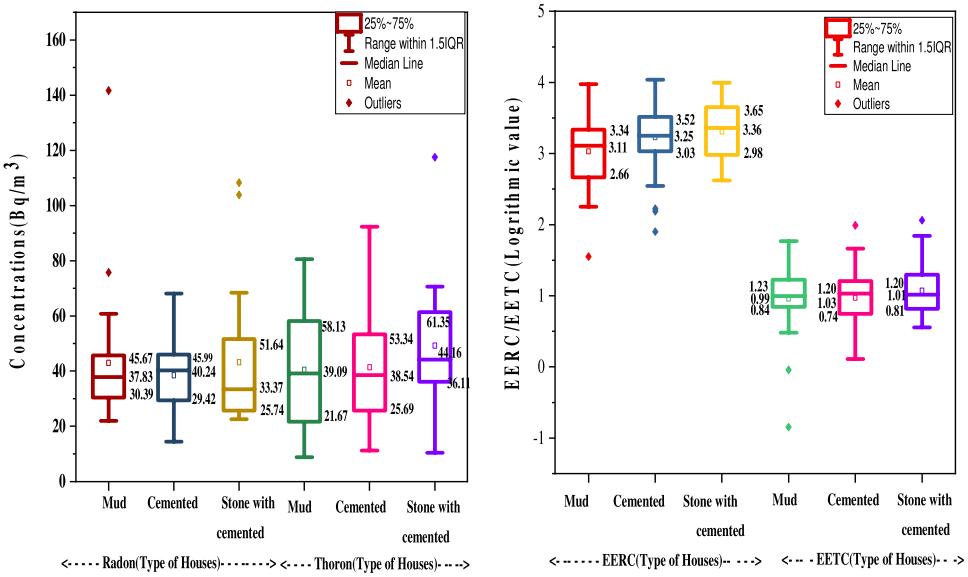

Fig. 6 **a** Box-Whisker plot of ^{222}Rn and ^{220}Rn variations. **b** Box-Whisker plot of EERC and EETC variations

It can be seen from Table 3, the GM for ^{222}Rn, ^{220}Rn and their decay products (EETC, EERC) can be observed to be varying in order of mud > stone > cement. Relatively high exhalation rates and radium/ thorium content (source term) for the soil (especially mud construction) can be attributed to higher values of ^{222}Rn, ^{220}Rn, EERC, and EETC. Lower concentration values in the cemented house can be related to the fact that the surfaces are coated with cement, resulting in decreased radiation inward flux, which affects interior concentration (Singh et al. 2016; Semwal et al. 2018, 2019). Besides, bare flooring (especially in stone houses) contributes towards higher flux/concentration in the dwellings.

Pie charts for ^{222}Rn and ^{220}Rn are also shown in Fig. 7 to dwell the effect of building material further. As can

Table 3 Statistical data of indoor ^{222}Rn, ^{220}Rn and their progeny for different types of dwellings

Statistical parameters	^{222}Rn			^{220}Rn			EERC			EETC		
	M	C	S	M	C	S	M	C	S	M	C	S
Range	24–69	15–56	23–59	18–107	10–68	10–68	9–43	12–36	15–37	0.17–3.90	0.14–0.85	0.21–2.65
RSD	0.27	0.29	0.31	0.45	0.36	0.39	0.37	0.26	0.24	0.48	0.43	0.48
GM, GSD	43, 1.33	33, 1.35	35, 1.35	46, 1.58	31, 1.45	37, 1.66	21, 1.47	21, 1.32	21, 1.24	1.67, 2.23	0.37, 1.54	1.36, 2.23

M mud, *C* cement, *S* stone with cement

be observed, ~ 63%, 36% and 32% of the mud, stone and cemented houses, respectively, showed ^{222}Rn concentration higher than global average (40 Bq/m^3). For EERC, 63%, 36% and 20% of the mud, stone and cemented houses, respectively, were reported having a concentration higher than its yearly average. For ^{220}Rn, 84% and 61% and 48% of the mud, stone and cemented houses, respectively, showed concentration values higher than its annual average of 34 Bq/m^3. Besides, 5% of the mud houses were observed with ^{220}Rn concentration higher than 100 Bq/m^3 (arbitrary reference). While EETC concentration was observed higher than its yearly average of 0.58 Bq/m^3 in 90%, 62% of the mud and stone houses, respectively. For cemented houses, 20% of houses were reported to have EETC higher than 0.58 Bq/m^3.

Implication from yearly data

After examining the effects of seasons and construction materials on observed concentration values, the complete year's data were aggregated for further analysis. Therefore, available 240 data points (three readings for each dwelling) were clustered for annual analysis. Figure 8 corresponds to the frequency distribution curve for ^{222}Rn and ^{220}Rn concentrations calculated annually. Table 4 lists statistical parameters such as concentration range, mean values, and standard deviation. Table 4 shows the values of annual concentration of ^{222}Rn lies in the range of 6 to 99 Bq/m^3 with GM (GSD) as 34 (1.65) Bq/m^3 which is relatively lesser to global average value of 40 Bq/m^3 (UNSCEAR 2000) while for ^{220}Rn lies in the range of 6–120 Bq/m^3 with GM (GSD) as 34 (1.78) Bq/m^3 which is significantly higher than the world average value of 10 Bq/m^3 (UNSCEAR 2000) and comparable to ^{222}Rn concentration value in the study region. EERC and EETC lie within the range of 3–56 Bq/m^3 with GM (GSD) as 21 (1.57) Bq/m^3 and 0.03 to 4.43 Bq/m^3 with GM (GSD) as 0.58 (3.41) Bq/m^3, respectively. The EERC and EETC values are reported bit higher than the worldwide average value of 10 and 0.02 Bq/m^3, respectively (UNSCEAR 2008, 2009).

A comparison of the current study's findings with those of other research conducted in different Indian regions was also carried out. Table 5 shows that the average concentrations of ^{222}Rn, ^{220}Rn, EERC and EETC observed in the study region are comparable to those found in other recent investigations (Bangotra et al. 2019; Kumar et al. 2020a; Ramola et al. 2016; Semwal et al. 2019).

Estimation of equilibrium factor (EF) and dose assessment

The estimation of equilibrium factor for ^{222}Rn, ^{220}Rn and their decay product is essential for dose assessment. With the invention of new techniques (DTPS/DRPS) to measure

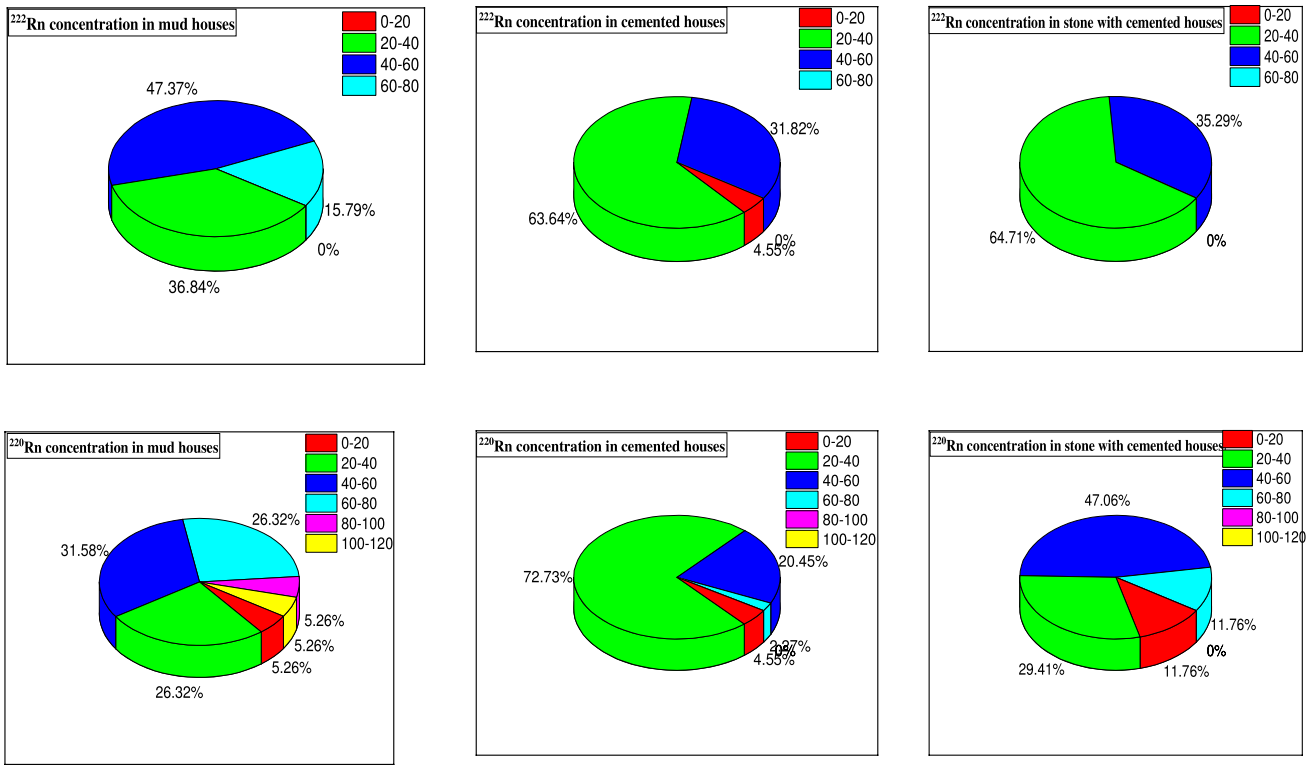

Fig. 7 The seasonal variation Pie chart of ^{222}Rn and ^{220}Rn concentration

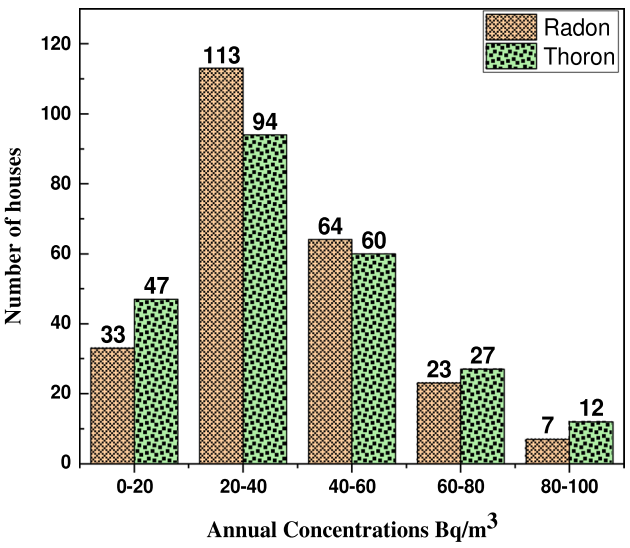

Fig. 8 Frequency Distribution curve for annual ^{222}Rn and ^{220}Rn concentration

Table 4 Annual statistical data of ^{222}Rn, ^{220}Rn and their progeny

Statistical parameters	^{222}Rn	^{220}Rn	EERC	EETC
Range	9–99	6–120	3–56	0.03–4.42
GM, GSD	34, 1.65	34, 1.78	21, 1.57	0.58, 3.41

^{222}Rn and ^{220}Rn progeny, it is easier to calculate the EF for ^{222}Rn and ^{220}Rn. Hence EF and annual effective doses (due to ^{222}Rn, ^{220}Rn and their decay products) are predicted for the study region using Eqs. 1–5 and tabulated in the form of Table 6.

EF for ^{222}Rn and its decay products was found to be varying from 0.28 to 0.77, yearly averaged value (i.e. 0.52) which is higher to the global reference value (0.4) (ICRP 1991; UNSCEAR 2000). On the other hand, EF for ^{220}Rn and its decay products was estimated (0.02) is comparable to the reference value (0.02) (UNSCEAR 2000) but with significant uncertainty.

The average effective dose attributed to ^{222}Rn and ^{220}Rn was 1.33 (1.34) and 0.20 (2.7) mSv/y, respectively. Annual inhalation dose (AID) due to ^{222}Rn, ^{220}Rn and their progeny was found to be 0.85–3.93 mSv/y with GM (GSD) as 1.71 (1.76) mSv/y. Data from Table 6 indicate the significant contribution of ^{220}Rn and its progeny to the annual inhalation dose.

Conclusion

This study presented the results of measurements of indoor ^{222}Rn, ^{220}Rn and their decay product activity levels in Nainital District of Uttarakhand, India. Measurements

Table 5 Comparison of results of present study with recent studies conducted for Indian regions

^{222}Rn concentration range (Bq/m^3), AM	^{220}Rn concentration range (Bq/m^3), AM	EERC, AM (Bq/m^3)	EETC, AM (Bq/m^3)	Location	References
24–98 (60)	46–689 (292)	–	–	Orissa	Ramola et al. (2013)
23–147 (57)	15–201 (66)	8–56(23)	.008–3.49(1.28)	Bagewshwar Uttarakhand	Kumar et al. (2020a)
44–157	44–240	10–63	1–5	Himachal Pradesh	Bajwa et al. (2016)
17–94(45.34)	14–125(44)	8–57	0.5–3.5	Punjab	Bangotra et al. (2019)
18–59(29)	30–204(85)	10–30(18)	1.1–2.1	Jammu & Kashmir	Kumar et al. (2020b)
27–148 (54)	5–174 (43)	7.6–48.6 (19.5)	0.6–4.6 (1.9)	Garhwal Himalaya	Ramola et al. (2016)
14–217(82)	5–213(65)	3–76 (26)	0.01–0.68 (0.24)	Almora, Uttarkhand	Semwal et al. (2019)
9–99 (34)	6–120 (34)	3–56 (21)	0.03–4.42 (0.58)	Nainital, Uttarakhand	Present Study

Table 6 Estimation of equilibrium factor and annual inhalation dose

	Equilibrium factor		Annual effective dose		AID (mSv/y)
	^{222}Rn & its progeny	^{220}Rn & its progeny	^{222}Rn & its progeny	^{220}Rn & its progeny	
Range	0.28–0.77	0.004–0.19	0.60–2.69	0.03–1.13	0.85–3.93
GM,GSD	0.52, 1.32	0.02, 2.4	1.33, 1.34	0.20, 2.7	1.71, 1.76

were taken in selected 80 houses situated at different altitudes. Single entry-based pin hole dosimeter and progeny sensors have been employed for the measurement of gases and decay products, respectively. The results have been interpreted on the basis of difference in building materials (mud, stone and cement) and seasonal variations (winter, summer and rainy). These were further utilized for deducing yearly averaged parameters and for performing dose calculations. Q–Q plots made for seasonal interpretations implied that ^{222}Rn and ^{220}Rn and their decay products follow a positive skewness towards the right tail. Wintertime values for ^{222}Rn, ^{220}Rn and EERC-EETC concentration were found to be higher than the corresponding values for summer and rainy season. These levels varied in the order of mud > stone > cement when the data were segregated on the basis of difference in building materials. Estimated yearly averaged equilibrium factor for the study region came out to be 0.52 and 0.02 for ^{222}Rn and its decay products and ^{220}Rn and its decay products, respectively. However large dispersion for the factor has been seen in the study region. Annual inhalation dose (AID) due to ^{222}Rn, ^{220}Rn and their progeny was found to be 0.85–3.93 mSv with GM (GSD) as 1.71 (1.76) mSv. The present study showed the significant contribution of ^{220}Rn and its progeny to the annual inhalation dose. It was also seen that in most of the mud houses, gases and their decay product's concentration remained significantly higher than their respective global average in the winter season. The concentration range, mean values were also compared with the other studies conducted in nearby regions. The results of this study follow the general conclusions of similar studies conducted in nearby region.

Acknowledgements The authors are thankful to Board of Research in Nuclear Science (BRNS), Department of Atomic Energy (DAE) Mumbai, India for providing the funds and the facilities for carrying out the research work.

Funding This work was supported by Board of Research in Nuclear Science (BRNS), Department of Atomic Energy (DAE) Mumbai, India [Project No. 2013/36/61-BRNS/2470].

Availability of data and materials The datasets used and/or analysed during the current study are available from the corresponding author on reasonable request.

Declarations

Conflict of interest The authors declare that they have no conflict of interest.

Ethical approval and consent to participate Not Applicable.

Consent for publication Not Applicable.

References

Agarwal TK, Sahoo BK, Gaware JJ, Joshi M, Sapra BK (2014) CFD based simulation of thoron (^{220}Rn) concentration in a delay chamber for mitigation application. J Environ Radioact 136:16–21

Agarwal TK, Joshi M, Sahoo BK, Kanse SD, Sapra BK (2015) Effect of ^{220}Rn gas concentration distribution on its transmission from

a delay chamber: evolving a CFD-based uniformity index. Radiat Prot Dosim 168:546–552
Agarwal TK, Sahoo BK, Joshi M, Mishra R, Meisenberg O, Tschiersch J, Sapra BK (2019) CFD simulations to study the effect of ventilation rate on ^{220}Rn concentration distribution in a test house. Radiat Phys Chem 162:82–89
Agarwal TK, Sahoo BK, Shetty T, Gaware JJ, Kumara S, Karunakara N et al (2020) Numerical simulation of ^{222}Rn profiling in an experimental chamber using CFD technique. J Environ Radioact 220:106298
Bajwa BS, Singh P, Singh P, Saini K, Singh S, Sahoo BK, Sapra BK (2016) A follow-up study on indoor ^{222} Rn, ^{220} Rn their decay product concentrations in a mineralised zone of Himachal Pradesh. India Radiat Prot Dosimetry 168:553–560. https://doi.org/10.1093/rpd/ncv367
Bangotra P, Mehra R, Kaur K, Jakhu R (2016) Study of natural radioactivity (^{226}Ra, ^{232}Th and ^{40}K) in soil samples for the assessment of average effective dose and radiation hazards. Radiat Prot Dosimetry 171(2):277–281
Bangotra P, Mehra R, Jakhu R, Pandit P, Prasad M (2019) Quantification of an alpha flux based radiological dose from seasonal exposure to ^{222}Rn, ^{220}Rn and their different EEC species. Sci Rep 9(1):1–15
Darby, S., Hill, D., Auvinen, A., Barros-Dios, J.M., Baysson, H., Bochicchio, F., Deo, H., Falk, R., Forastiere, F., Hakama, M., Heid, I., Kreienbrock, L., Kreuzer, M., Lagarde, F., Mkelinen, I., Muirhead, C., Oberaigner, W., Pershagen, G., Ruano- Ravina, A., Ruosteenoja, E., Schaffrath Rosario, A., Tirmarche, M., TomBek, L., Whitley, E., Wichmann, H.E., Doll, R., 2005. Radon in homes and risk of lung cancer: collaborative analysis of individual data from 13 European case-control studies. BMJ 223–330.
Dowdall A, Murphy P, Pollard D, Fenton D (2017) Update of Ireland's national average indoor radon concentration–application of a new survey protocol. J Environ Radioact 169:1–8
Hu J, Yang G, Hegedűs M, Iwaoka K, Hosoda M, Tokonami S (2018) Numerical modeling of the sources and behaviors of ^{222}Rn, ^{220}Rn and their progenies in the indoor environment—A review. J Environ Radioact 189:40–47
IAEA TEC DOC 1450, 2005. Thorium Fuel Cycle d Potential Benefits and Challenges. IAEA, Vienna.
ICRP (1991) Recommendations of the International Commission on Radiological Protection. ICRP Publication 60 (Anals of the ICRP 21)
ICRP (International Commission on Radiological Protection) (2014) Radiological protection against radon exposure. ICRP Publication 126, Annals of the ICRP, 43(3).
Joshi M, Sapra BK, Kothalkar P, Khan A, Modi R, Mayya YS (2011) Implications of polarity of unipolar ionisers on reduction of effective dose attributable to thoron progeny. Radiat Prot Dosimetry 145(2–3):256–259
Kandari T, Prasad M, Pant P, Semwal P, Bourai AA, Ramola RC (2018) Study of radon flux and natural radionuclides (^{226}Ra, ^{232}Th and ^{40}K) in the Main Boundary Thrust region of Garhwal Himalaya. Acta Geophys 66(5):1243–1248
Karunakara N, Yashodhara I, Kumara KS, Tripathi RM, Menon SN, Kadam S, Chougaonkar MP (2014) Assessment of ambient gamma dose rate around a prospective uranium mining area of South India–a comparative study of dose by direct methods and soil radioactivity measurements. Results in Physics 4:20–27
Karunakara N, Shetty T, Sahoo BK, Kumara KS, Sapra BK, Mayya YS (2020) An innovative technique of harvesting soil gas as a highly efficient source of ^{222}Rn for calibration applications in a walk-in type chamber: part-1. Sci Rep 10(1):1–5
Kaur M, Kumar A, Mehra R, Mishra R (2018) Dose assessment from exposure to radon, thoron and their progeny concentrations in the dwellings of sub-mountainous region of Jammu & Kashmir, India. J Radioanal Nucl Chem 315(1):75–88
Krewski D, Lubin JH, Zielinski JM, Alavanja M, Catalan VS, Field RW (2005) A combined analysis of North American case-control studies of residential 222Rn and lung cancer. Epidemiology 16:146–154
Kumar A, Singh P, Agarwal T, Joshi M, Semwal P, Singh K, Ramola RC (2020a) Statistical inferences from measured data on concentrations of naturally occurring radon, thoron, and decay products in Kumaun Himalayan belt. Environ Sci Pollut Res 27(32):40229–40243
Kumar A, Vij R, Sharma S, Sarin A (2020b) Seasonal variation of indoor radon/thoron and their progeny levels in lesser-Himalayas of Jammu & Kashmir, India. J Radioanal Nucl Chem 323(1):495–506
Kumara KS, Sahoo BK, Gaware JJ, Sapra BK, Mayya YS, Karunakara N (2017) Thoron mitigation system based on charcoal bed for applications in thorium fuel cycle facilities (part 2):development, characterization, and performance evaluation. J Environ Radioact 172:249–260
Meisenberg O, Mishra R, Joshi M, Gierl S, Rout R, Guo L, Agarwal T, Kanse S, Irlinger J, Sapra BK, Tschiersch J (2016) Radon and thoron inhalation doses in dwellings with earthen architecture : Comparison of measurement methods. Sci Total Environ 579:1855–1862. https://doi.org/10.1016/j.scitotenv.2016.11.170
Milner J, Chalabi Z, Wilkinson P, Armstrong B, Cairns J, Das P et al (2014) Evidence review and economic analysis of excess winter deaths. Review 1: Factors determining vulnerability to winter-and cold-related mortality/morbidity. National Institute for Health and Care Excellence, London
Mishra R, Mayya YS (2008a) Study of a deposition-based direct thoron progeny sensor (DTPS) technique for estimating equilibrium equivalent thoron concentration (EETC) in indoor environment. Radiat Meas 43(8):1408–1416
Mishra R, Mayya YS (2008b) Study of a deposition-based direct thoron progeny sensor (DTPS) technique for estimating equilibrium equivalent thoron concentration(EETC) in indoor environment. Radiation Measurement 43:1408–1416. https://doi.org/10.1016/j.radmeas.2008.03.002
Mishra R, Mayya YS, Kushwaha HS (2009a) Measurement of 220Rn/222Rn progeny deposition velocities on surfaces and their comparison with theoretical models. J Aerosol Sci 40:1–15. https://doi.org/10.1016/j.jaerosci.2008.08.001
Mishra R, Sapra BK, Mayya YS (2009b) Nuclear Instruments and Methods in Physics Research B Development of an integrated sampler based on direct 222Rn/220Rn progeny sensors in flow-mode for estimating unattached / attached progeny concentration. Nucl Inst Methods Phys Res B 267:3574–3579. https://doi.org/10.1016/j.nimb.2009.08.021
Mishra R, Prajith R, Sapra BK, Mayya YS (2010) Nuclear Instruments and Methods in Physics Research B Response of direct thoron progeny sensors (DTPS) to various aerosol concentrations and ventilation rates. Nucl Inst Methods Phys Res B 268:671–675. https://doi.org/10.1016/j.nimb.2009.12.012
Mishra R, Zunic ZS, Venoso G, Bochicchio F, Stojanovska Z, Carpentieri C et al (2014) An evaluation of thoron (and radon) equilibrium factor close to walls based on long-term measurements in dwellings. Radiat Prot Dosimetry. https://doi.org/10.1093/rpd/ncu083
Omori Y, Shimo M, Janik M, Ishikawa T, Yonehara H (2020) Variable strength in thoron interference for a diffusion-type radon monitor depending on ventilation of the outer air. Int J Environ Res Public Health 17(3):974
Prajith R, Rout RP, Kumbhar D, Mishra R, Sahoo BK, Sapra BK (2019) Measurements of radon (^{222}Rn) and thoron (^{220}Rn) exhalations

and their decay product concentrations at Indian Stations in Antarctica. Environmental Earth Sciences 78(1):35

Prasad Y, Prasad G, Gusain GS, Choubey VM, Ramola RC (2008) Radon exhalation rate from soil samples of South Kumaun Lesser Himalayas, India. Radiat Meas 43:369–374

Prasad M, Rawat M, Dangwal A, Kandari T, Gusain GS, Mishra R, Ramola RC (2016a) Variability of radon and thoron equilibrium factors in indoor environment of Garhwal Himalaya. J Environ Radioact 151:238–243

Prasad M, Rawat M, Dangwal A, Prasad G, Mishra R, Ramola RC (2016b) Study of indoor radon, thoron and progeny in the indoor environment of Yamuna and Tons valleys of Garhwal Himalaya and progeny in the indoor environment of yamuna. Radiat Prot Dosimetry 171(2):187–191

Prasad M, Bossew P, Kumar GA, Mishra R, Ramola RC (2018a) Dose assessment from the exposure to attached and unattached progeny of radon and thoron in indoor environment. Acta Geophys 66(5):1187–1194

Prasad M, Kumar GA, Sahoo BK, Ramola RC (2018b) A comprehensive study of radon levels and associated radiation doses in Himalayan groundwater. Acta Geophys 66(5):1223–1231

Ramola RC, Prasad M (2020) Significance of thoron measurements in indoor environment. J Environ Radioact 225:106453

Ramola RC, Rautela BS, Gusain GS, Prasad G, Sahoo SK, Tokonami S (2013) Measurements of radon and thoron concentrations in high radiation background area using pin-hole dosimeter. Radiat Meas 53–54:71–73

Ramola, R.C., Prasad, M., Kandari, T., Pant, P., Bossew, P., Mishra, R.,Tokonami, S., 2016. Dose estimation derived from the exposure to radon , thoron and their progeny in the indoor environment. Scientific Reports, 6.

Sahoo BK, Sapra BK, Gaware JJ, Kanse SD, Mayya YS (2011) A model to predict radon exhalation from walls to indoor air based on the exhalation from building material samples. Sci Total Environ 409(13):2635–2641

Sahoo BK, Sapra BK, Kanse SD, Gaware JJ, Mayya YS (2013) A new pin-hole discriminated ^{222}Rn/^{220}Rn passive measurement device with single entry face. Radiat Meas 58:52–60

Semwal P, Agarwal TK, Singh K, Joshi M, Gusain GS, Sahoo BK, Ramola RC (2019) Indoor inhalation dose assessment for thoron rich regions of Indian Himalayan belt. Environ Sci Pollut Res 26(5):4855–4866

Semwal P., Singh K., Agarwal TK., Joshi M., Pant P., Kandari T., Ramola RC., 2018. Measurement of ^{222}Rn and ^{220}Rnexhalation rate from soil samples of Kumaun Hills, India. Acta Geophys:1–9

Sharma S, Kumar A, Mehra R, Kaur M, Mishra R (2018) Assessment of progeny concentrations of ^{222}Rn/^{220}Rn and their related doses using deposition-based direct progeny sensors. Environ Sci Pollut Res 8:1–4

Shetty T, Mayya YS, Kumara KS, Sahoo BK, Sapra BK, Karunakara N (2020) A periodic pumping technique of soil gas for 222 Rn stabilization in large calibration chambers: part 2—theoretical formulation and experimental validation. Sci Rep 10(1):1–1

Singh K, Semwal P, Pant P, Gusain GS, Joshi M, Sapra BK, Ramola RC (2016) Measurement of radon, thoron and their progeny in different types of dwelling in Almora district of Kumaun Himalayan region. Radiat Prot Dosimetry 171:223–228

Sinha AK. Himalayan Geology. 1977 volume 7, Published by Wadia Institute

Trilochana S, Somashekarappa HM, Kumara KS, Mayya YS, Karunakara N (2020) CFD-based simulation and experimental verification of 222 Rn distribution in a walk-in type calibration chamber. J Radioanal Nucl Chem 323(1):507–513

United Nations Scientific Committee on the Effects of Atomic Radiation (UNSCEAR), 1993. Report to the General Assembly, with scientific annexes. United Nations, New York.

United Nations Scientific Committee on the Effect of Atomic Radiation (UNSCEAR),2010.Sources and Effects of Ionizing Radiation. UNSCEAR 2008 Report Volume I: Sources. United Nations, New York.

United Nations Scientific Committee on the Effect of Atomic Radiation(UNSCEAR) (2008) Sources and effects of ionizing radiation. United Nations, New York

United Nations Scientific Committee on the Effects of Atomic Radiation (UNSCEAR), 2000.Sources and Effects of Ionizing Radiation.UNSCEAR 2000 Report Volume I: Sources. United Nations, New York.

United Nations Scientific Committee on the Effects of Atomic Radiation (UNSCEAR), 2009. UNSCEAR 2006 Report. Sources to Effects Assessment for Radon in Homes and Workplaces, vol. II (Annex E).

Valdiya KS. Geology of kumaun lesser Himalaya. Wadia Institute of Himalayan Geology; 1980

Wang F, Ward IC (2002) Radon entry, migration and reduction in houses with cellars. Build Environ 37:1153–1165

World Health Organization (WHO) (2009) Hand book on indoor radon: a public health perspective. WHO Press, Geneva